# Carrier dynamics in individual concentric quantum rings: Photoluminescence measurements

S. Sanguinetti
*L-NESS and Dipartimento di Scienza dei Materiali, Universitá di Milano Bicocca, Via Cozzi 53, I-20125 Milano, Italy*

M. Abbarchi, A. Vinattieri, M. Zamfirescu, and M. Gurioli
*LENS and Dipartimento di Fisica, Universitá di Firenze, Via Sansone 1, I-50019 Sesto Fiorentino, Italy*

T. Mano, T. Kuroda, and N. Koguchi*
*National Institute for Materials Science, 1-2-1 Sengen, Tsukuba, Ibaraki 305-0047, Japan*
(Received 3 September 2007; published 7 March 2008)

We present a detailed analysis of the emission of individual GaAs/AlGaAs concentric quantum rings. Time resolved and excitation power density dependence of the photoluminescence has been used in order to determine the carrier dynamics in concentric quantum rings. Despite the small spatial separation between the two rings of the concentric quantum ring complex, the exciton dynamics in the two rings is completely decoupled. A significant increase in the emission width and rise time, with respect to the quantum dot case, characterize the emission of the rings. We attribute such phenomenology to the exciton center-of-mass localization induced by ring height fluctuations in quantum-wire-like fashion.

DOI: 10.1103/PhysRevB.77.125404 PACS number(s): 78.67.−n, 73.21.−b, 78.55.Cr

Self-assembled semiconductor quantum dots (QDs) are currently intensively investigated because of their potential as building blocks for optoelectronic devices such as nanoemitters and for quantum information technologies[1–4] associated with the remarkable similarity of QDs with atomic systems. Several promising applications in these fields, such as single photon source for quantum cryptography,[1] quantum bits,[4] or quantum logical elements,[3,4] require the coherent manipulation of the carrier population in the adjacent QDs. The possibility to control the coupling between different QDs and the understanding of the carrier recombination dynamics in those nanostructures are therefore topics of extreme relevance.

Recent experimental works have achieved the formation of very peculiar artificial diatomic molecules made of self-assembled, strain-free, concentrically coupled GaAs/AlGaAs quantum rings.[5] The electronic level distribution of these nanostructures has been attributed to exciton confinement in either the inner or the outer ring[5,6] by means of cw-photoluminescence (PL) measurements. The single-electron[6] and electron-hole[7,8] energy levels, also in a magnetic field, were studied theoretically, showing that, even if the electron and hole wave functions are mainly confined in the inner ring (IR) or in the outer ring (OR) (depending on the energy), tunneling effects on the carrier dynamics cannot be excluded *a priori*. However, the electronic coupling between states in the inner and outer rings has not been addressed experimentally, even if, for their possible use in quantum nanodevices, the determination of the effective carrier dynamics in the concentric quantum rings (CQRs) is very important.

In this paper, we report detailed measurements of time resolved photoluminescence of individual CQRs as a function of the excitation power density $P_{exc}$. We clearly found that the recombination kinetics of carriers in the inner and outer rings are decoupled. This stays true also at large carrier injection, where the PL of each ring evolves in independent multiplets, which is a clear signature of multiexcitonic emission. We conclude that exciton localization effects dominate the radiative recombination rate in CQRs.

GaAs CQRs were grown on $Al_{0.3}Ga_{0.7}As$ using droplet epitaxy.[9–11] In droplet epitaxy, cation (Ga) atoms are supplied solely in the initial stage of growth, producing nanometer-sized droplets of Ga clusters. After the formation of the Ga droplets, anion atoms (As) are supplied, leading to crystallization of the droplets into GaAs nanocrystals. In contrast to the other methods of fabricating QDs, such as Stranski–Krastanow growth, this technique can produce strain-free quantum dots based on lattice-matched heterosystems. Droplet epitaxy allows for a high controllability of the crystalline shape, via the As flux, from conelike to CQR structures characterized by an inner and an outer ring.[5] The CQR sample here studied was obtained by depositing Ga droplets [1.75 monolayer (ML) of Ga at 0.05 ML/s on the surface of an $Al_{0.3}Ga_{0.7}As$ substrate at 300 °C] followed by irradiation with $2\times10^{-6}$ Torr beam equivalent pressure of As at 200 °C. The CQR has been characterized before capping by atomic force microscopy (AFM), as shown in Fig. 1. The CQRs show good circular symmetry, whereas a small elongation is found along the $(01\bar{1})$ direction (5% for the inner ring and 8% for the outer ring). The inner ring dimensions are 40 nm diameter with 6 nm height, and the outer ring dimensions are 80 nm diameter with 5 nm height, respectively. The CQR density is $1.3\times10^{8}$ $cm^{-2}$, thus allowing the capture of the emission from a single CQR structure using a micro-objective setup. After ring formation, the sample was capped by an $Al_{0.3}Ga_{0.7}As$ barrier of 100 nm thickness. A thick (Al,Ga)As layer completes the structure. The samples underwent a rapid thermal annealing (RTA) at 750 °C for 4 min to improve their optical quality. Note that the final RTA processing does not modify the nanocrystalline ring shape, according to the negligible interdiffusion of Ga and As at a GaAs/(Al,Ga)As heterointerface at the relevant temperature.[12]

We performed time resolved measurements for several

 

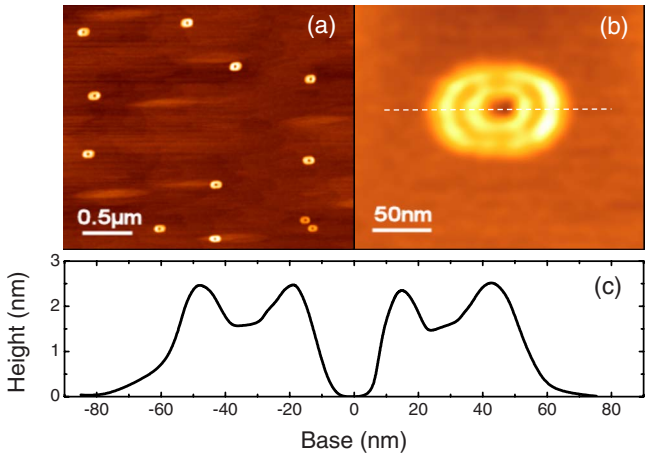


FIG. 1. (Color online) [(a) and (b)] AFM images of an uncapped CQR sample. (c) AFM profile of the single CQR in (b) taken along the dashed line.

different single CQRs under nonresonant excitation in the AlGaAs barrier. The sample was placed in a cold-finger helium flow cryostat, and $\mu$PL measurements were performed in the far field using a microscope objective (numerical aperture of 0.5). A dye laser pumped by the second harmonic of a Nd:YAG pulsed laser was used as the excitation source at a wavelength of 600 nm; the pulse duration was 5 ps with a repetition rate of 76 MHz and $P_{exc}$ in the range $1-100$ W/cm$^2$. For the collection, a confocal configuration of two infinity corrected microscope objectives was used. The PL signal was then focused to a monomode optical fiber with a core diameter of 3.5 $\mu$m, assuring a lateral resolution of 0.7 $\mu$m, and dispersed by a single grating spectrometer. The signal was detected by a Peltier cooled charge coupled device, for time integrated measurements, and by a microchannel photomultiplier with a time correlated single photon counting setup, for time resolved measurements. The spectral resolution was 0.2 meV and the time resolution, after standard deconvolution procedures, was below 20 ps.

Figure 2 reports the typical photoluminescence spectrum of an individual CQR. The emission spectrum of an individual CQR is always a doublet, whose components are separated by a few meV (see Table I). The width of each single line in the doublet is close to 1 meV, ranging from 1.1 meV of CQR1 to 0.8 meV of CQR3. These values are very large for individual nanostructures and it has to be attributed to inhomogeneous broadening mechanisms. It is also worth noting that the spectral diffusion of the PL line associated with chargeable defects near the nanostructure, commonly assumed for explaining the single QD broadening in the range of a few hundred $\mu$eV, seems hardly the explanation for our 1 meV broadening. The doublet structure of the emission has been attributed by Ref. 5 to the emissions of the IR and of the OR of the CQR, respectively, based on the effective mass model. The IR line corresponds to the high energy line emission, while the OR emission, due to its lower lateral confinement, is the lower energy line of the doublet. The energy separation of the lines in the doublet varies depending on the individual CQR considered and, within the

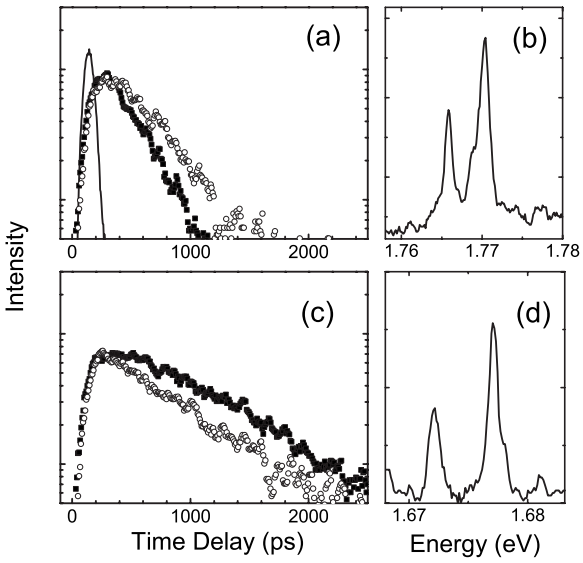


FIG. 2. (a) Time resolved PL, at $T=10$ K and $P_{exc}=10$ W/cm$^2$, of CQR2. Open circles indicate OR emission, full squares IR emission. (b) PL spectrum of CQR2 at $T=10$ K and $P_{exc}=10$ W/cm$^2$. (c) Time resolved PL, at $T=10$ K and $P_{exc}=3$ W/cm$^2$, of CQR3. Open circles indicate OR emission, full squares IR emission. (d) PL spectrum of CQR2 at $T=10$ K and $P_{exc}=1$ W/cm$^2$.

model predictions, it depends on the values of the radii of the IR and of the OR.[6]

Figure 2 also reports the time resolved emission, at low $P_{exc}$, of the two lines of different CQR doublets. Four different CQRs were measured. The rise time of the IR and OR lines of different CQR doublets is almost the same ($\tau_R=120\pm40$ ps) in all the investigated CQRs. This value is about four times larger than the commonly measured $\tau_R$ for quantum dot structures, even in the case of GaAs/AlGaAs quantum dots.[13] On the other hand, the PL lifetimes $\tau_D$ show large variations for the individual ring considered (see Table I). This spread of $\tau_D$ is possibly due to different shapes and sizes of the CQRs[14] or, more likely, to the presence of nonradiative channels, since there is no clear correlation with the emission energy of the CQR. More important is the fact that although small differences (within 30%) were observed between IR and OR $\tau_D$s, the two lifetimes are quite similar for each pair of rings, even if, as stressed before, the overall lifetime varies by more than a factor of 4 for different CQRs. Note also that sometimes the IR decays faster than the OR and sometimes is the opposite.

TABLE I. Emission energies ($E_{PL}$) and decay times ($\tau_D$) of the measured IR and OR lines at $T=10$ K and $P_{exc}=3$ W/cm$^2$.

| | IR | | OR | |
|---|---|---|---|---|
| | $E_{PL}$ (eV) | $\tau_D$ (ps) | $E_{PL}$ (eV) | $\tau_D$ (ps) |
| CQR1 | 1.709 | $200\pm50$ | 1.704 | $220\pm60$ |
| CQR2 | 1.770 | $230\pm50$ | 1.766 | $350\pm100$ |
| CQR3 | 1.672 | $900\pm100$ | 1.667 | $700\pm100$ |
| CQR4 | 1.795 | $600\pm100$ | 1.789 | $900\pm200$ |

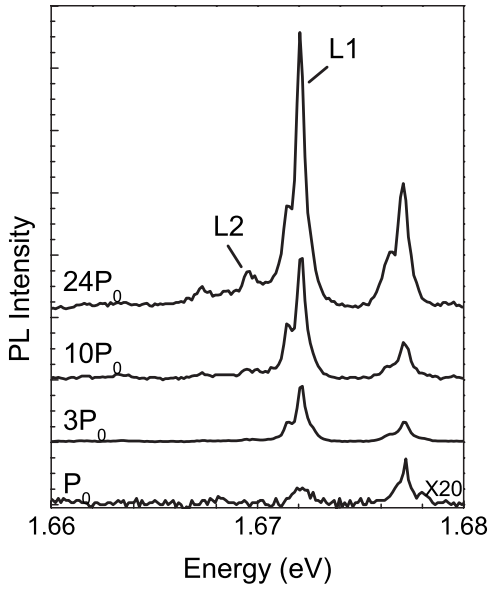


FIG. 3. Time integrated spectra of CQR3 at different excitation power densities. $T=10$ K and $P_0=3$ W/cm$^2$.

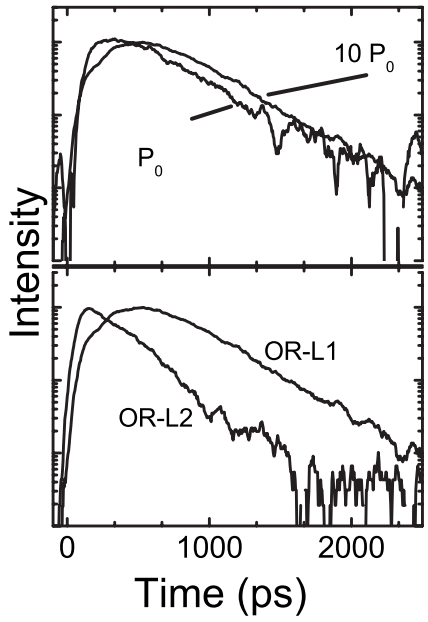


FIG. 4. Top panel: Time resolved PL of the OR line of CQR3 at $T=10$ K and at different $P_{\mathrm{exc}}$. ($P_0=3$ W/cm$^2$). Bottom panel: Time resolved PL of the single exciton (L1 in Fig. 3) and the multiexciton (L2 in Fig. 3) line of the OR of CQR3, respectively. $P_{\mathrm{exc}}=10P_0$ and $T=10$ K.

Further insights on possible coupling mechanisms between CQR excited states may be found by performing state filling experiments. The dependence of the CQR emission on $P_{\mathrm{exc}}$ is shown in Fig. 3 for CQR3. Both IR and OR lines show a superlinear dependence of the PL integrated intensity on $P_{\mathrm{exc}}$. Above 10 W/cm$^2$, both IR and OR lines evolve to multiplets, with new lines appearing on the low energy side of the fundamental transitions, whose relative intensities grow much faster, with $P_{\mathrm{exc}}$, than the fundamental ones. The energy separation between the lines in the multiplets ranges from $\approx$2 meV (OR case) to $\approx$1 meV (IR case). More information on the nature of the multiplets' origin can be gained by means of time resolved PL measurements as a function of $P_{\mathrm{exc}}$, as reported in Fig. 4. Strong increases of the PL rise times of the fundamental optical transition are found when increasing the power density, due to state filling condition. At high $P_{\mathrm{exc}}$, correlated dynamics is observed between two lines corresponding to the multiplet which originates from the OR line at high $P_{\mathrm{exc}}$ (lines L1 and L2 in Fig. 4). The rise time of line L1 corresponds to the decay time of line L2, thus demonstrating a link between the carrier population in the two states. Such correlation between decay and rise times stems from states which are bound in a cascadelike behavior. The observed energy differences, the relative dependencies on $P_{\mathrm{exc}}$, and the interlinked carrier dynamics of the lines in the OR multiplet allow us to attribute the L1 and L2 emissions to single and multiexciton recombination from the OR ground state, closely resembling the QD case.[15–17] As far as the carrier dynamics is concerned, the IR fundamental line shows a similar behavior, denoting an independent state filling mechanism with respect to the OR case, even if the cascadelike dynamics in the IR multiplet is partially hidden by the presence of the OR recombination on the low energy side of the IR line.

Let us now discuss the experimental data on the framework of possible carrier tunneling and/or transfer between the two concentric quantum rings. The overall phenomenology presented here clearly excludes the picture of a carrier transfer between IR and OR, and we then conclude that the recombination kinetics of carriers in the inner and outer rings are decoupled. In fact, whether the carrier dynamics in the two structures were in some way correlated, a hierarchical order in the PL decay should be observed, with the shorter decay time belonging to the higher state, denoting a cascade mechanism associated with the carrier relaxation paths. On the contrary, the IR recombination lifetime is always larger than the rise time of the OR time resolved emission. Moreover, almost the same decay times are observed in IR and OR recombination for each CQR, even if large variations are observed for different CQRs.

Similar conclusions can be obtained by the analysis of carrier dynamics under a large optical injection. For both IR and OR emissions, we observe the increase of rise times when increasing $P_{\mathrm{exc}}$. This is clear evidence of saturation effects associated with state filling conditions. This type of dynamics is illustrated by the lines L1 and L2 present at high $P_{\mathrm{exc}}$ in the emission of the OR of CQR3. In this case, the $\tau_D$ of L2 corresponds to the rise time of L1, implying that the two emissions come from energy states connected in a cascade-type dynamics, where the higher states in the ladder act as feeders of the ground state. As we stated before, the L1 and L2 lines of the OR multiplet are attributed to single and multiexciton recombination. Their emission energy difference stems from a different occupation of the ring, which changes the number of spectator excitons from several (line L2) to zero (line L1), thus making the dynamics of two lines strictly correlated. At the same time, if we compare the time dependence of the IR and OR at $P_{\mathrm{exc}}=70$ W/cm$^2$ lines, we cannot find any correlation between rise and decay times of the emission, thus showing that the carrier dynamics in the

two rings is decoupled. Therefore, as already stated before, we have experimentally proven that the photoinjected carriers follow independent relaxation paths within the electronic level structures of the two CQRs, in agreement with the assumptions made in Ref. 6, on the basis of cw-PL measurements. Such decoupling of the carrier kinetics happens despite the proximity of the two rings in a CQR structure. If we suppose that the excitons are free to move over the whole ring, the lack of coupling between the two rings could be traced back to the lack of resonance conditions between states having the same angular momentum values inside the IR and OR. However, other effects, such as we see in the following, may play a role.

As a matter of fact, as far as the energy relaxation efficiency of the electron-hole pairs photogenerated in the quantum rings is concerned, it should be noted that the low $P_{\mathrm{exc}}$ measurements show relatively large values of $\tau_R$ compared to the QD case. This suggests a less effective relaxation channel in the CQR compared to the QD case. This happens despite the much closer spacing of the ring states, which should prevent the appearance of a phonon-bottleneck effect. These quite controversial considerations, linked with the puzzling large broadening of 1 meV of the PL lines, suggested to us to consider a different explanation of the presented phenomena. Quantum rings, due to their rather peculiar annular shape, possess an electronic structure which is a crossover between the dot and the wire cases,[6] since the linear extension of a ring of 80 nm diameter is already quite large (250 nm). Thus, quantum rings can be considered as a warped analog of quantum wires (QWi's). In the QWi, confinement energy fluctuations, whose magnitude is significantly lower than the exciton binding energy,[18] due to QWi size disorder, take place. The presence of such disorder principally affects the exciton center-of-mass (c.m.) part of the exciton wave function, giving rise to states with a spatially localized c.m. motion. The presence of exciton c.m. localized states has strong effects on the optical properties of the QWi, the more evident is, naturally, the inhomogeneous broadening of the emission lines, which is linked to the exciton energy disorder. In addition to this, the exciton c.m. localization in the QWi induces a serious reduction of the phonon scattering rates.[18] At the same time, the kinetics of excitons in a landscape scenario of localized states induced by disorder is well known to produce an increase of the emission rise time associated with the exciton motion toward the state of minimum energy, in agreement with the experimental findings. The effect of the exciton c.m. localization on the coupling of OR and IR is twofold. On one hand, excitonic c.m. localization partially relaxes the angular momentum conservation in exciton transitions, thus making possible the coupling between the two rings. However, on the other hand, by increasing the average spatial separation between the exciton states, which are localized in small regions of the rings, it strongly reduces the probability of tunneling between states belonging to OR and IR, in agreement with our experimental results.

In conclusion, we carefully analyzed the time and $P_{\mathrm{exc}}$ dependence of the PL emission of individual CQRs. We conclude that, despite the small spatial separation between the two rings of the CQR complex, the carrier relaxation dynamics and the exciton kinetics in the IR and OR are decoupled. Moreover, a significant increase of the emission full width at half maximum and rise time $\tau_R$, with respect to the QD case, has been observed. We attribute the observed phenomenology to the exciton c.m. localization induced by structural disorder along the ring.

This work was partially supported by the Italian PRIN-MIUR contract No. 2006022932 and by the CARIPLO Foundation through the QUADIS Project.

*Present address: L-NESS and Dipartimento di Scienza dei Materiali, Universitá di Milano Bicocca, Via Cozzi 53, I-20125, Milano, Italy.

[1] P. Michler, A. Kiraz, C. Becher, W. V. Schoenfeld, P. M. Petroff, L. Zhang, E. Hu, and A. Imamoglu, Science **290**, 2282 (2000).
[2] R. M. Stevenson, R. M. Thompson, A. J. Shields, I. Farrer, B. E. Kardynal, D. A. Ritchie, and M. Pepper, Phys. Rev. B **66**, 081302(R) (2002).
[3] X. Li, Y. Wu, D. Steel, D. Gammon, T. H. Stievater, D. S. Katzer, D. Park, C. Piermarocchi, and L. J. Sham, Science **301**, 809 (2003).
[4] P. Solinas, P. Zanardi, N. Zanghi, and F. Rossi, Phys. Rev. B **67**, 121307(R) (2003).
[5] T. Mano *et al.*, Nano Lett. **5**, 425 (2005).
[6] T. Kuroda, T. Mano, T. Ochiai, S. Sanguinetti, K. Sakoda, G. Kido, and N. Koguchi, Phys. Rev. B **72**, 205301 (2005).
[7] J. Planelles and J. I. Climente, Eur. Phys. J. B **48**, 65 (2005).
[8] J. I. Climente, J. Planelles, M. Barranco, F. Malet, and M. Pi, Phys. Rev. B **73**, 235327 (2006).
[9] N. Koguchi, S. Takahashi, and T. Chikyow, J. Cryst. Growth **111**, 688 (1991).
[10] N. Koguchi and K. Ishige, Jpn. J. Appl. Phys., Part 1 **32**, 2052 (1993).
[11] K. Watanabe, N. Koguchi, and Y. Gotoh, Jpn. J. Appl. Phys., Part 2 **39**, L79 (2000).
[12] T. E. Schlesinger and T. Kuech, Appl. Phys. Lett. **49**, 519 (1986).
[13] S. Sanguinetti, K. Watanabe, T. Tateno, M. Wakaki, N. Koguchi, T. Kuroda, F. Minami, and M. Gurioli, Appl. Phys. Lett. **81**, 613 (2002).
[14] M. Abbarchi, M. Gurioli, S. Sanguinetti, M. Zamfirescu, A. Vinattieri, and N. Koguchi, Phys. Status Solidi C **3**, 3860 (2006).
[15] T. Kuroda, S. Sanguinetti, M. Gurioli, K. Watanabe, F. Minami, and N. Koguchi, Phys. Rev. B **66**, 121302(R) (2002).
[16] E. Dekel, D. Gershoni, E. Ehrenfreund, J. M. Garcia, and P. M. Petroff, Phys. Rev. B **61**, 11009 (2000).
[17] E. Dekel, D. V. Regelman, D. Gershoni, E. Ehrenfreund, W. V. Schoenfeld, and P. M. Petroff, Phys. Rev. B **62**, 11038 (2000).
[18] A. Feltrin, J. L. Staehli, B. Deveaud, and V. Savona, Phys. Rev. B **69**, 233309 (2004).